Environmental and Experimental Botany 162 (2019) 383–391

Contents lists available at ScienceDirect

Environmental and Experimental Botany

journal homepage: www.elsevier.com/locate/envexpbot

Substituting green or far-red radiation for blue radiation induces shade avoidance and promotes growth in lettuce and kale

Qingwu Meng, Nathan Kelly, Erik S. Runkle*

Department of Horticulture, Michigan State University, 1066 Bogue Street, East Lansing, MI, 48824-1325, USA

ARTICLE INFO

Keywords:
Controlled-environment agriculture
Cryptochrome
Phytochrome
Shade-avoidance response
Sole-source lighting

ABSTRACT

Although red (R; 600–700 nm) and blue (B; 400–500 nm) radiation can be sufficient for plants grown indoors, other wavebands such as green (G; 500–600 nm) and far red (FR; 700–800 nm) can also regulate photosynthesis, plant morphology, and secondary metabolism. The objective of this study was to determine how substitutions of B radiation with G and/or FR radiation influence growth of leafy greens grown indoors under light-emitting diodes (LEDs). We postulated G and/or FR radiation (and low B radiation) would trigger shade-avoidance responses and thus promote biomass accumulation through increased radiation interception. We grew lettuce (*Lactuca sativa* 'Rex' and 'Rouxai') and kale (*Brassica oleracea* var. *sabellica* 'Siberian') under warm-white (WW) LEDs at 180 $\mu mol \cdot m^{-2} \cdot s^{-1}$ (400–800 nm) for 9–11 days and then transplanted seedlings into a hydroponic system with ten different lighting treatments. The air temperature (20 °C), photoperiod (20 h), total photon flux density (180 $\mu mol \cdot m^{-2} \cdot s^{-1}$; 400–800 nm), and fertility were maintained the same across treatments. In addition to WW and equalized-white (EQW) controls, combinations of B (peak = 449 nm), G (peak = 526 nm), and FR (peak = 733 nm) LEDs, each at 0, 20, 40, or 60 $\mu mol \cdot m^{-2} \cdot s^{-1}$, were delivered in a R background (peak = 664 nm) of 120 $\mu mol \cdot m^{-2} \cdot s^{-1}$. One month after seed sow, we collected data on shoot mass, leaf morphology, and pigmentation. Substituting G or FR radiation for B radiation promoted leaf expansion and increased shoot mass but decreased chlorophyll concentrations in all crops. For example, lettuce 'Rex' grown under 60 $\mu mol \cdot m^{-2} \cdot s^{-1}$ of G + 120 $\mu mol \cdot m^{-2} \cdot s^{-1}$ of R radiation was 38% greater in plant diameter and 54% greater in shoot dry mass compared to those under 60 $\mu mol \cdot m^{-2} \cdot s^{-1}$ of B + 120 $\mu mol \cdot m^{-2} \cdot s^{-1}$ of R radiation. Substituting B radiation with G radiation at 60 $\mu mol \cdot m^{-2} \cdot s^{-1}$ also reduced red coloration of lettuce 'Rouxai'. At the same photon flux density, FR radiation increased leaf expansion and decreased red foliage coloration more than G radiation. We conclude that substituting G and/or FR radiation for B radiation triggers shade-avoidance responses, accelerating plant growth while decreasing pigment concentrations.

1. Introduction

Radiation is both an energy source and a signal to higher plants. Biologically relevant wavelengths from ultraviolet to far-red (FR; 700–800 nm) radiation create an energy gradient, the variation of which enables plants to sense and survive in various environmental conditions. Photosynthetically active radiation, by definition, ranges from 400 to 700 nm and includes blue (B; 400–500 nm), green (G; 500–600 nm), and red (R; 600–700 nm) radiation. Light-emitting diode (LED) fixtures developed for horticultural applications have generally been comprised of B + R radiation because of their high photosynthetic and electrical efficacy. In contrast, G LEDs are rarely included in sole-source lighting mainly because they are highly inefficient due to physical challenges in optoelectronics. Green radiation is perceived as less useful to plant growth than B and R radiation because of its weaker absorption by chlorophylls; however, it has a higher quantum yield than B radiation (McCree, 1972). In addition, a substantial amount (70–80%) of G radiation is absorbed by the leaf (McCree, 1972; Brodersen and Vogelmann, 2010). Moreover, G radiation penetrates deeper in the leaf profile than B or R radiation, scatters between cellular components within the leaf, and drives photosynthesis through abundant lower chloroplasts (Sun et al., 1998; Terashima et al., 2009; Brodersen and Vogelmann, 2010).

Green radiation can evoke shade-avoidance responses such as

Abbreviations: B, blue; EQW, equalized white; FR, far red; G, green; LED, light-emitting diode; PIF, phytochrome-interacting factor; PPE, phytochrome photoequilibrium; PPFD, photosynthetic photon flux density; R, red; TPFD, total photon flux density; W, white; WW, warm white; YPFD, yield photon flux density

* Corresponding author.
E-mail addresses: mengqin1@msu.edu (Q. Meng), runkleer@msu.edu (E.S. Runkle).

https://doi.org/10.1016/j.envexpbot.2019.03.016
Received 18 December 2018; Received in revised form 14 March 2019; Accepted 15 March 2019
Available online 15 March 2019
0098-8472/

promotion of hypocotyl elongation, stem extension, leaf expansion, and hyponasty (Zhang et al., 2011; Wang and Folta, 2013). It can also reverse B radiation-induced responses such as inhibition of extension growth, stimulation of stomata opening, and promotion of anthocyanin accumulation (Folta, 2004; Folta and Maruhnich, 2007; Wang and Folta, 2013). Green radiation increased shoot mass and extension growth in some studies. For example, a partial substitution of R radiation (from LEDs if unspecified hereinafter) with 24% G radiation (from fluorescent lamps) in a 16%B + 84%R background at a photosynthetic photon flux density (PPFD; 400–700 nm) of 150 $\mu mol \cdot m^{-2} \cdot s^{-1}$ increased shoot fresh and dry mass and leaf area of lettuce (*Lactuca sativa*) 'Waldmann's Green' (Kim et al., 2004a). In addition, substituting G radiation (peak = 516 nm) for B radiation in a 50%B + 50%R background at a PPFD of 160 $\mu mol \cdot m^{-2} \cdot s^{-1}$ increased shoot fresh mass of tomato (*Solanum lycopersicum*); shoot dry mass of petunia (*Petunia* × *hybrida*); height of impatiens (*Impatiens walleriana*), tomato, and salvia (*Salvia splendens*); and leaf area of tomato (Wollaeger and Runkle, 2014). In contrast, G radiation did not influence crop growth and morphology in other studies. For example, shoot dry mass, net assimilation (dry mass per unit leaf area), and specific leaf area of lettuce 'Waldmann's Green' were similar under varying G radiation percentages from 2% to 41% at a PPFD of 200 or 500 $\mu mol \cdot m^{-2} \cdot s^{-1}$ (Snowden et al., 2016). Moreover, shoot mass and leaf size of baby leaf lettuce 'Red Cross' were similar when 43% of cool-white (W) fluorescent radiation was substituted with 130 $\mu mol \cdot m^{-2} \cdot s^{-1}$ G radiation (peak = 526 nm), which increased G radiation percentage of the PPFD from 52% to 70% (Li and Kubota, 2009).

Far-red radiation is outside the PPFD waveband but can also drive photochemistry and photosynthesis, although the quantum yield of FR radiation is low (McCree, 1972; Pettai et al., 2005; Zhen and van Iersel, 2017). The radiation-dependent reaction of photosynthesis begins with excitation of photosystem II preferentially by slightly shorter wavelengths (≤ 680 nm) followed by excitation of photosystem I preferentially by slightly longer wavelengths (≥ 700 nm). Simultaneous delivery of FR radiation with B + R or W radiation helps prevent overexcitation of photosystem II and balance electron flow in the photosynthetic machinery, thereby increasing the quantum yield of photosystem II (Myers, 1971; Zhen and van Iersel, 2017). As a signal, FR radiation can also modulate phytochrome activity and thus control a wide range of photomorphogenic responses. It converts phytochromes to their inactive form (Pr), whereas R radiation converts them to their active form (Pfr) (Sager et al., 1988). The addition of FR radiation can elicit shade-avoidance responses through phytochromes, modifying stem and leaf morphology, and increase growth of baby leaf lettuce and various ornamental seedlings (Li and Kubota, 2009; Park and Runkle, 2017).

Both G and FR radiation mediate photosynthesis and shade-avoidance responses; however, a knowledge gap exists with respect to their comparative and cumulative effects. Moreover, the increasing popularity of W LEDs in horticultural lighting necessitates testing of multi-waveband combinations for indoor production of specialty crops. The objective of our study was to investigate how substitutions of G and/or FR radiation for B radiation influence shoot mass, morphology, and pigmentation of leafy greens. We postulated G and/or FR radiation, when substituted for B radiation, would increase shoot mass and extension growth, and decrease pigment concentrations.

2. Materials and methods

2.1. Plant material and propagation

Seeds of green butterhead lettuce 'Rex', red oakleaf lettuce 'Rouxai', and kale (*Brassica oleracea* var. *sabellica*) 'Siberian' were obtained from a seed producer (Johnny's Selected Seeds, Winslow, ME) and sown in a soilless rockwool substrate arranged as 200 2.5-cm plugs per sheet (AO 25/40 Starter Plugs; Grodan, Milton, ON, Canada), which was presoaked in deionized water with an adjusted pH of 4.4–4.5 using diluted (1:31) 95–98% sulfuric acid (J.Y. Baker, Inc., Phillipsburg, NJ). This experiment was performed three times with seeds of lettuce 'Rouxai' sown on 26 June, 4 Sept., and 19 Oct. 2017, and seeds of lettuce 'Rex' and kale 'Siberian' sown 2 d later in each replication. Seed plugs were placed in plastic trays and covered with transparent humidity domes to prevent seed desiccation during germination. The humidity domes were subsequently removed 4 d after seed sow. Seeds and seedlings were germinated and grown in a ventilated and refrigerated growth compartment in the Controlled-Environment Lighting Laboratory (Michigan State University, East Lansing, MI) at an air temperature setpoint of 20 °C and ambient CO_2 under a 24-h photoperiod and a total photon flux density (TPFD; 400–800 nm) of 180 $\mu mol \cdot m^{-2} \cdot s^{-1}$ from warm-white (WW; peak = 639 nm, correlated color temperature = 2700 K) LEDs (PHYTOFY RL; OSRAM, Beverley, MA). Seedlings were irrigated with deionized water supplemented with a water-soluble fertilizer (13N–3P–15 K Orchid RO Water Special, 12.5% nitrate nitrogen and 0.7% ammoniacal nitrogen; Greencare Fertilizers, Inc., Kankakee, IL) to supply the following nutrients (in $mg \cdot L^{-1}$): 100 N, 23 P, 115 K, 62 Ca, 15 Mg, 1.4 Fe, 0.68 Mn, 0.34 Zn, 0.14 B, 0.34 Cu, and 0.14 Mo. The electrical conductivity ranged from 1.0 to 1.2 $mS \cdot cm^{-1}$. pH was routinely adjusted to 5.5–5.8 using potassium bicarbonate.

2.2. Production culture and environment

All lettuce and kale seedlings in rockwool cubes were transplanted into a deep-flow hydroponic system with three vertically stacked layers (Indoor Harvest, Houston, TX) on 7 July, 15 Sept., and 30 Oct. 2017 for three replications to receive ten different lighting treatments. The plants were spaced on 20-cm horizontal and 15-cm diagonal centers on 36-cell floating rafts (60.9 × 121.9 × 2.5 cm; Beaver Plastics, Ltd; Acheson, AB, Canada). They were grown at an air temperature setpoint of 20 °C and ambient CO_2 under a 20-h photoperiod (0200–2200 HR) with roots fully submerged in constantly recirculating deionized water supplemented with the same water-soluble fertilizer as for seedlings to supply the following nutrients (in $mg \cdot L^{-1}$): 150 N, 35 P, 173 K, 92 Ca, 23 Mg, 2.0 Fe, 1.0 Mn, 0.51 Zn, 0.21 B, 0.51 Cu, and 0.21 Mo. The pH [5.8 ± 0.3 (standard deviation) to 5.9 ± 0.3 in replication one, 5.6 ± 0.3 to 5.8 ± 0.3 in replication two, and 5.9 ± 0.3 to 6.1 ± 0.4 in replication three], electrical conductivity (in $mS \cdot cm^{-1}$; 1.30 ± 0.07 to 1.38 ± 0.07 in replication one, 1.67 ± 0.11 to 1.82 ± 0.06 in replication two, and 1.54 ± 0.09 to 1.59 ± 0.08 in replication three), and temperature of the nutrient solutions (in °C; 20.6 ± 0.2 to 22.0 ± 0.2 in replication one, 21.8 ± 0.2 to 23.6 ± 0.6 in replication two, and 20.9 ± 0.2 to 21.8 ± 0.2 in replication three) for all lighting treatments were measured daily throughout the experiment with a pH and electrical conductivity meter (HI9814; Hanna Instruments, Woonsocket, RI). The nutrient solution was constantly oxygenated with an air stone (20.3 × 2.5 cm; Active Aqua AS8RD; Hydrofarm, Petaluma, CA) and a 60-W air pump (Active Aqua AAPA70 L; Hydrofarm).

Ventilation and air-conditioning units (HBH030A3C20CRS; Heat Controller, LLC., Jackson, MI) ran on a wireless thermostat controller (Honeywell International, Inc., Morris Plains, NJ) to promote air flow (up to an air flow rate of 0.9 $m \cdot s^{-1}$ from in-unit fans) and maintain the air temperature setpoint. Thermocouples (0.13-mm type E; Omega Engineering, Inc., Stamford, CT), infrared temperature sensors (OS36-01-K-80 F; Omega Engineering, Inc.), light quantum sensors (LI-190R; LI-COR, Inc., Lincoln, NE), CO_2 sensors (GMD20; Vaisala, Inc., Louisville, CO), and relative humidity and temperature probes (HMP110; Vaisala, Inc.) were used to monitor corresponding environmental parameters. One or two sensors of each type were positioned in representative locations of the growth room. These environmental data were collected once every 10 s with hourly averages recorded using a datalogger (CR1000; Campbell Scientific, Inc., Logan, UT) coupled with

a multiplexer (AM16/32B; Campbell Scientific, Inc.). Environmental data for all lighting treatments throughout the experiment were taken from their closest sensors and ranged from 20.0 ± 0.2 (standard deviation) to 21.2 ± 1.0 °C for air temperature, from 379 ± 22 to 402 ± 41 ppm for CO_2 concentration, and from 44% ± 3% to 58% ± 12% for relative humidity.

2.3. Lighting treatments

From transplant to harvest, plants were grown under ten different lighting treatments consisting of B (peak = 449 nm), G (peak = 526 nm), R (peak = 664 nm), FR (peak = 733 nm), WW, and equalized-white (EQW; peak = 559 nm, 6500 K) LEDs, which were all housed in the same adjustable LED fixture with seven independent color channels (PHYTOFY RL; OSRAM). The radiation output of each color channel is controlled at 1-μmol·m^{-2}·s^{-1} increments using proprietary software (Spartan Control Software; OSRAM). Three LED fixtures (67.3 × 29.8 × 4.3 cm each) were positioned 43 cm above each treatment canopy and spaced on 41-cm centers to ensure radiation uniformity. All lighting treatments delivered the same TPFD of 180 μmol·m^{-2}·s^{-1} from WW, EQW, or constant R radiation at 120 μmol·m^{-2}·s^{-1} with eight combinations of B, G, and FR radiation supplying the remaining 60 μmol·m^{-2}·s^{-1}: $B_{60}R_{120}$, $B_{40}G_{20}R_{120}$, $B_{20}G_{40}R_{120}$, $G_{60}R_{120}$, $B_{40}R_{120}FR_{20}$, $B_{20}R_{120}FR_{40}$, $R_{120}FR_{60}$, $B_{20}G_{20}R_{120}FR_{20}$, WW_{180}, and EQW_{180}. The number following each waveband indicates its photon flux density in μmol·m^{-2}·s^{-1}. All LEDs were scheduled in the control software to run the designated spectral combinations for 20 h d^{-1}. The spectral distributions of all lighting treatments were measured using a portable spectroradiometer (PS200; Apogee Instruments, Inc., Logan, UT) and adjusted in the control software based on the TPFD averaged from seven representative locations, where individual plants were located on the floating raft (Table 1, Fig. 1). The yield photon flux density (YPFD) was the product of the spectral data and relative quantum efficiency from 350 to 800 nm (McCree, 1972) (Table 1). The estimated phytochrome photoequilibrium (PPE) was calculated as the proportion of FR-absorbing, active phytochromes in the total phytochrome pool based on the spectral data and absorption coefficients of phytochromes (Sager et al., 1988) (Table 1).

2.4. Data collection and analysis

Photographs of a representative plant under each lighting treatment were taken under white fluorescent light to document visual appearance (Fig. 2). Immediately after, destructive measurements were conducted on 10 plants per cultivar from each treatment and replication approximately 30 d after seed sow. For each plant, shoot fresh and dry mass, plant diameter, length and width of the fifth most mature leaf, leaf area (only collected for kale), petiole length (only collected for kale), and leaf number were measured. Shoots were dried in an oven (Blue M, Blue Island, IL) at 60 °C for 5 d before dry mass measurements. Moisture content was calculated as the fraction of the difference between fresh and dry mass in fresh mass. The net assimilation rate of kale was calculated as shoot dry mass per unit leaf area. Mean relative specific chlorophyll concentration was determined using a chlorophyll meter (SPAD-502; Konica Minolta Sensing, Inc., Chiyoda, Tokyo, Japan). The SPAD readings were subsequently converted to chlorophyll concentrations (in μmol·m^{-2}) based on equations from Parry et al. (2014). A Lab color space analysis was conducted with a colorimeter (Chroma Meter CR-400; Konica Minolta Sensing, Inc.) on lettuce 'Rouxai' to quantify foliage coloration. L^* ranges from 0 (the darkest black) to 100 (the brightest white) to indicate lightness. With the true neutral gray being 0, a^* is the scale of green (in the negative direction) to red (in the positive direction), whereas b^* is the scale of blue (in the negative direction) to yellow (in the positive direction).

The experiment was a randomized complete block design with time as the block. All data from three replications were combined and analyzed with the PROC MEANS, PROC MIXED, and PROC GLIMMIX procedures and Tukey's honestly significant difference test ($\alpha = 0.05$) in SAS (version 9.4; SAS Institute, Inc., Cary, NC) as well as linear regression ($\alpha = 0.05$) in SigmaPlot (version 12.5; Systat Software, Inc., San Jose, CA).

3. Results

3.1. Shoot mass

Shoot fresh mass of the two lettuce cultivars and kale decreased as the B photon flux density increased from 0 to 60 μmol·m^{-2}·s^{-1} under G or FR light (Fig. 3). The magnitude of the decrease was higher under G light (42%) than under FR light (27%) for lettuce 'Rex' but similar under G or FR light for lettuce 'Rouxai' (44% vs. 48%) and kale (33% vs. 30%), indicating spectral sensitivity varied among species and cultivars. When B radiation was substituted with the same photon flux density of G or FR radiation, shoot fresh mass of all crops was similar, except it was 26% higher under $G_{60}R_{120}$ than under $R_{120}FR_{60}$ for lettuce 'Rex'. Shoot fresh mass was also similar when lettuce and kale were grown under 20 μmol·m^{-2}·s^{-1} of B radiation and 40 μmol·m^{-2}·s^{-1} of G,

Table 1
Spectral characteristics of ten lighting treatments comprised of mixtures of blue (B; 400–500 nm), green (G; 500–600 nm), red (R; 600–700 nm), and far-red (FR; 700–800 nm); warm-white (WW); or equalized-white (EQW) light-emitting diodes. Integrated parameters include the photosynthetic photon flux density (PPFD; 400–700 nm), the total photon flux density (TPFD; 400–800 nm), and the yield photon flux density [YPFD; the product of relative quantum efficiency (McCree, 1972) and spectral data from 350 to 800 nm]. The estimated phytochrome photoequilibrium (PPE) was calculated as the proportion of active phytochromes in the total phytochrome pool according to Sager et al. (1988). The number following each waveband is its photon flux density in μmol·m^{-2}·s^{-1}.

	$B_{60}R_{120}$	$B_{40}G_{20}R_{120}$	$B_{20}G_{40}R_{120}$	$G_{60}R_{120}$	$B_{40}R_{120}FR_{20}$	$B_{20}R_{120}FR_{40}$	$R_{120}FR_{60}$	$B_{20}G_{20}R_{120}FR_{20}$	WW_{180}	EQW_{180}
Single-band photon flux density (μmol·m^{-2}·s^{-1})										
B	58.3	41.1	19.8	3.5	40.3	20.2	0.2	20.2	12.1	15.7
G	0.6	20.9	38.7	59.4	0.9	0.8	0.4	19.9	53.6	107.2
R	115.1	119.3	118.1	118.5	115.4	116.3	116.0	116.6	101.3	50.4
FR	1.0	1.2	1.2	1.3	21.1	41.4	58.0	21.3	18.8	6.2
Integrated photon flux density (μmol·m^{-2}·s^{-1})										
PPFD	174.1	181.4	176.6	181.4	156.6	137.3	116.6	156.7	166.9	173.3
TPFD	175.1	182.6	177.9	182.7	177.7	178.7	174.6	178.0	185.7	179.4
YPFD	150.9	158.5	155.3	159.5	141.6	130.6	117.4	142.9	153.0	153.4
Radiation ratio										
R:FR	112.7	98.1	95.0	93.0	5.5	2.8	2.0	5.5	5.4	8.2
B:R	0.5	0.3	0.2	0.0	0.3	0.2	0.0	0.2	0.1	0.3
B:G	90.0	2.0	0.5	0.1	44.0	24.8	0.4	1.0	0.2	0.1
B:FR	57.2	33.8	15.9	2.8	1.9	0.5	0.0	0.9	0.6	2.5
PPE	0.872	0.876	0.879	0.883	0.837	0.807	0.784	0.843	0.829	0.850

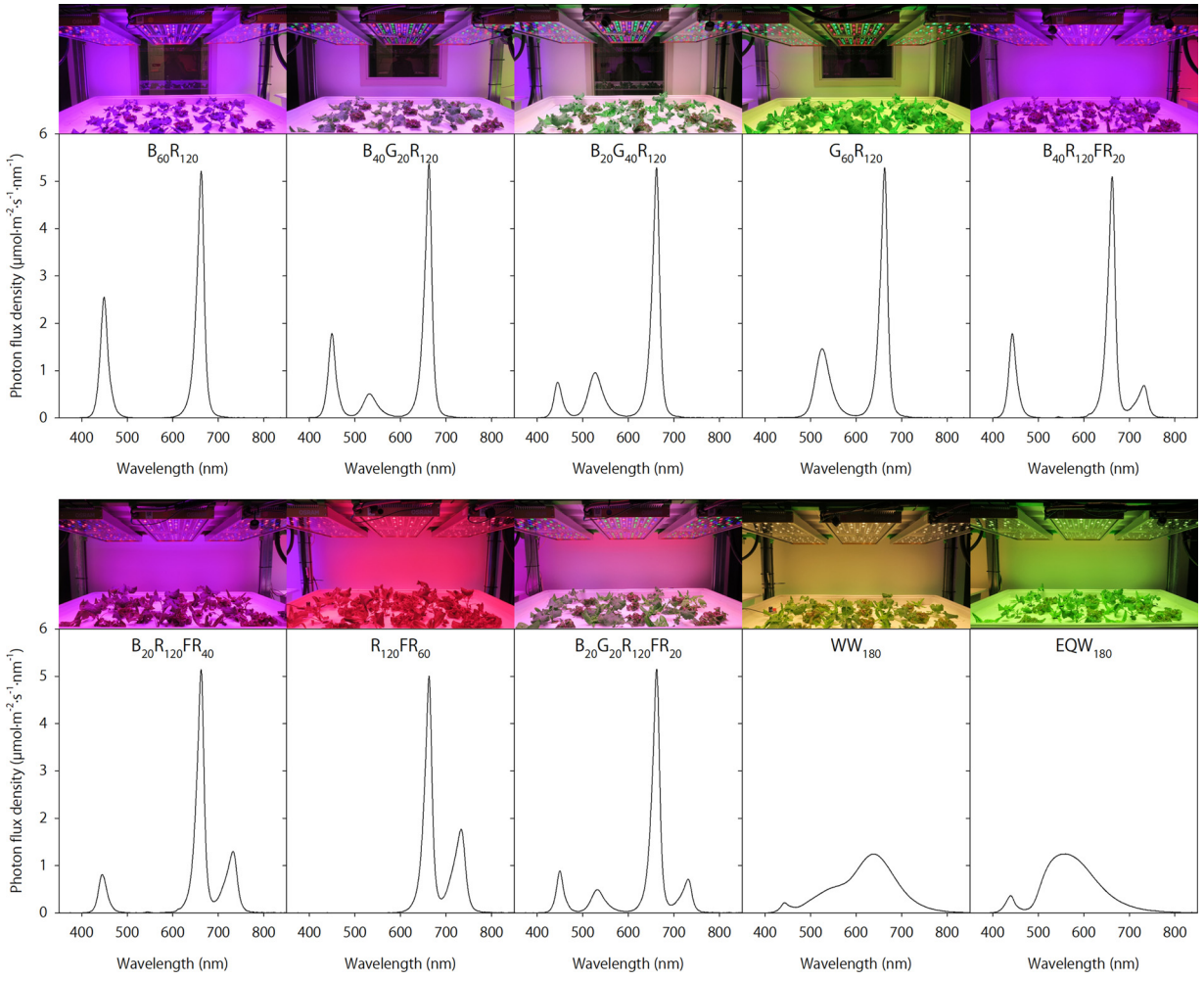

Fig. 1. Spectral distributions of ten lighting treatments comprised of mixtures of blue (B; 400–500 nm), green (G; 500–600 nm), red (R; 600–700 nm), and far-red (FR; 700–800 nm); warm-white (WW); or equalized-white (EQW) light-emitting diodes. The number following each waveband is its photon flux density in $\mu mol \cdot m^{-2} \cdot s^{-1}$ (For color visualization of the treatments, the reader is referred to the web version of this article).

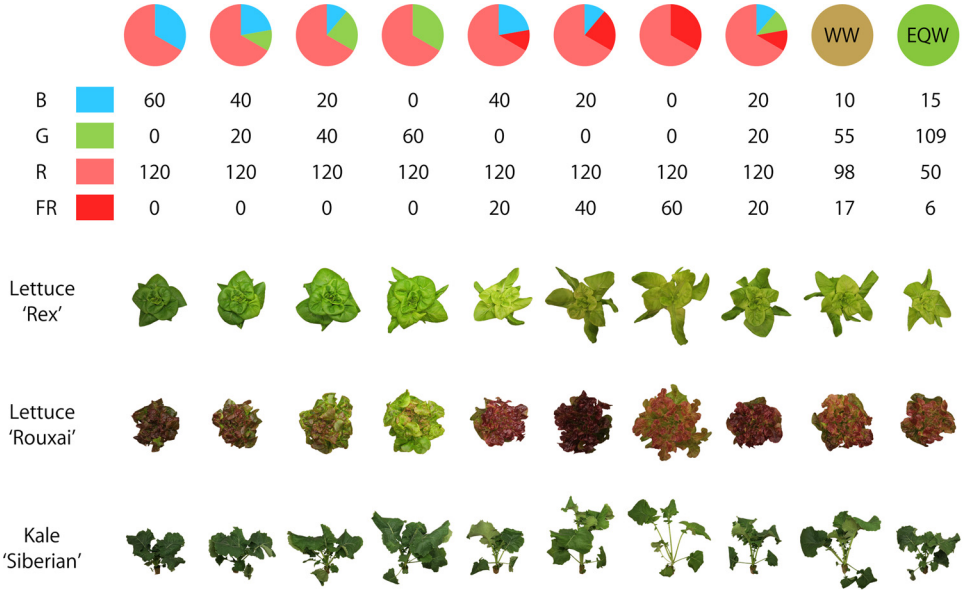

Fig. 2. Lettuce 'Rex' and 'Rouxai' 27 and 30 d after sowing, respectively. Plants were grown under ten lighting treatments comprised of mixtures of blue (B; 400–500 nm), green (G; 500–600 nm), red (R; 600–700 nm), and far-red (FR; 700–800 nm); warm-white (WW); or equalized-white (EQW) light-emitting diodes. The number for each waveband is its photon flux density in $\mu mol \cdot m^{-2} \cdot s^{-1}$ (For interpretation of the references to colour in this figure legend, the reader is referred to the web version of this article).

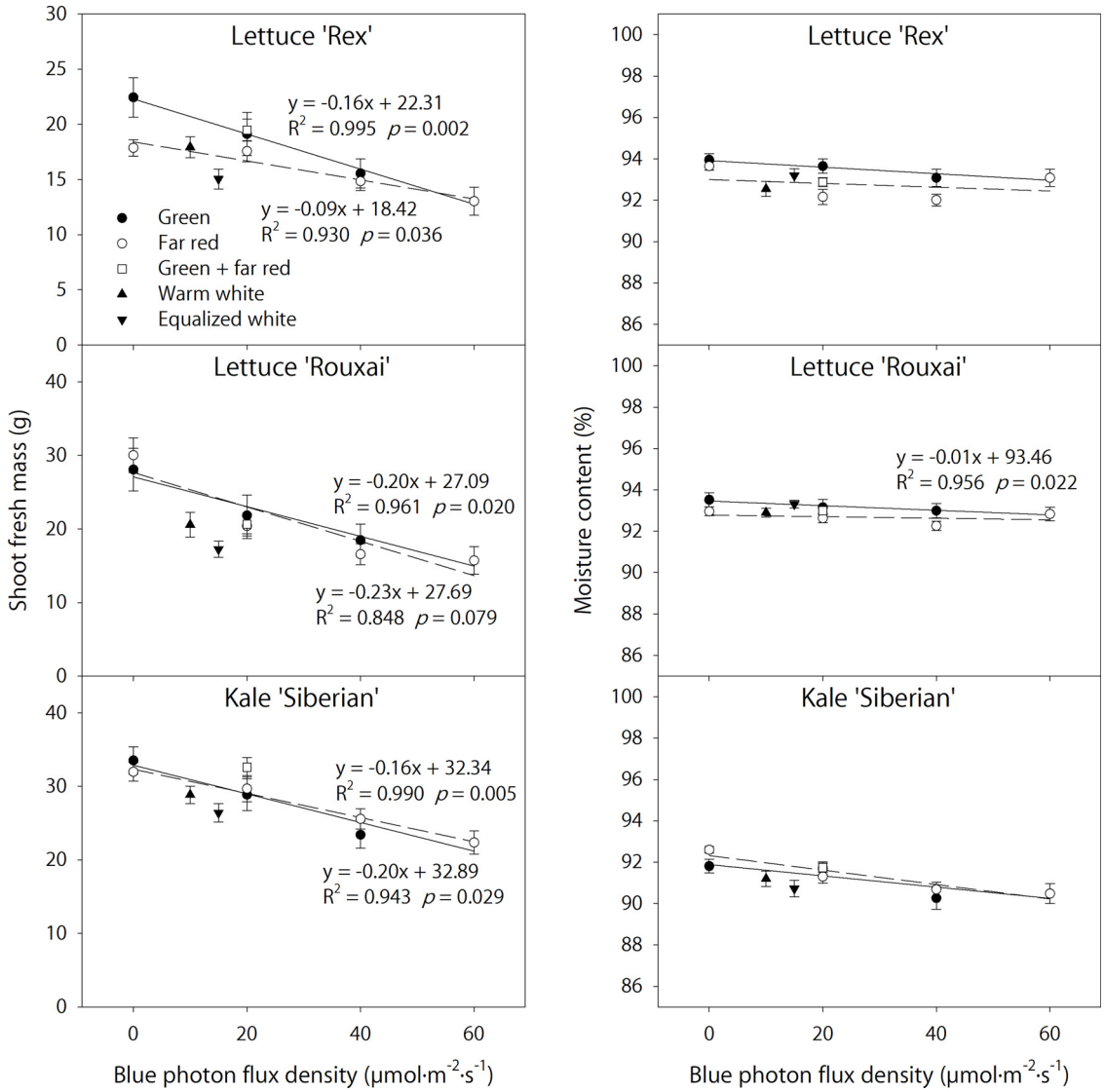

Fig. 3. Shoot fresh mass and moisture content of lettuce and kale. Plants were grown under ten lighting treatments comprised of mixtures of blue (B; 400–500 nm), green (G; 500–600 nm), red (R; 600–700 nm), and far-red (FR; 700–800 nm); warm-white (WW); or equalized-white (EQW) light-emitting diodes. Equations, coefficients of determination (R^2), and p-values are given for linear relationships ($\alpha = 0.05$) under G- (solid lines) and FR-substituted (dashed lines) treatments.

FR, or G + FR radiation, further showing similar effects of G and FR radiation under B radiation. Responses of shoot fresh and dry mass were generally similar (data of shoot dry mass not shown). Under G or FR radiation, moisture content of all crops was not influenced by B radiation except a 0.7% decrease for lettuce 'Rouxai' grown under G radiation as the B photon flux density increased from 0 to 60 $\mu mol \cdot m^{-2} \cdot s^{-1}$ (Fig. 3).

3.2. Plant morphology

Leaf length and width of all crops and leaf area and petiole length of kale, decreased as G or FR radiation was substituted with increasing B radiation (Fig. 4). For leaf length of lettuce and petiole length of kale, the magnitude of the decrease was higher under FR radiation than under G radiation, indicating greater sensitivity to FR radiation than G radiation in elongation responses. Both lettuce cultivars had similar responses of leaf length and plant diameter, which were positively correlated (Fig. 5). When the B photon flux density was fixed, kale grown under FR radiation had similar leaf area but longer petioles than under G radiation (Figs. 2 and 4). Blue radiation did not influence the net assimilation rate of kale under G or FR radiation (Fig. 4). As the B photon flux density increased from 0 to 60 $\mu mol \cdot m^{-2} \cdot s^{-1}$, the ratio of leaf length to width decreased with decreasing FR radiation for both lettuce cultivars, increased with decreasing G radiation for lettuce 'Rouxai', and did not change for kale (Fig. 4). In particular, leaves of lettuce 'Rex' grown under FR radiation appeared excessively elongated (Fig. 2).

3.3. Relationships between plant morphology and shoot mass

Shoot fresh mass positively correlated with plant diameter for both lettuce cultivars or leaf area for kale (Fig. 5). Slopes of linear regression lines were steeper under G radiation than under FR radiation. At the same shoot fresh mass, lettuce grown under FR radiation was larger in size than under G radiation, indicating less compactness under FR radiation. In contrast, relationships between leaf area and shoot fresh mass of kale were similar under G and FR radiation.

3.4. Leaf number, chlorophyll concentration, and foliage coloration

Leaf number of lettuce and kale was not influenced by the B photon flux density, except it decreased by one for lettuce 'Rex' grown under G radiation as the B photon flux density increased from 0 to

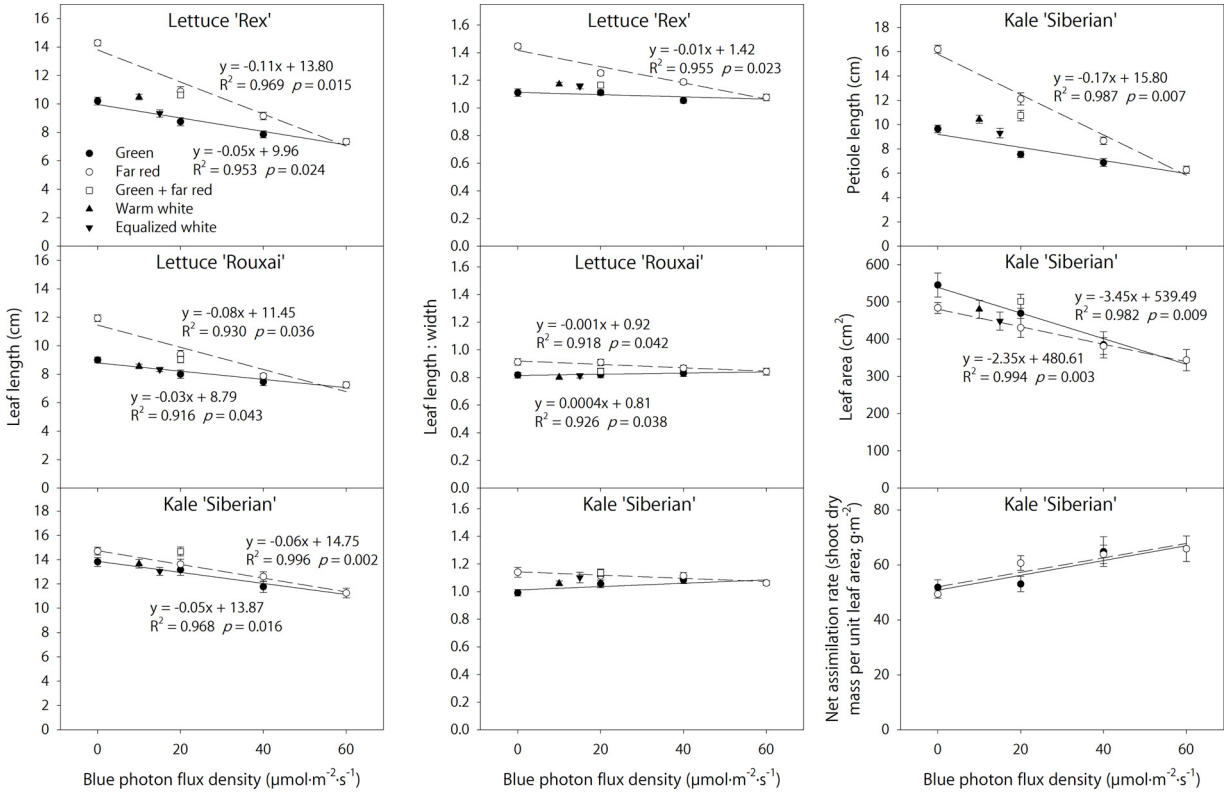

Fig. 4. Leaf length and the ratio of leaf length to width (leaf length : width) of the fifth most mature leaf of lettuce and kale and petiole length, leaf area, and net assimilation rate of kale. Plants were grown under ten lighting treatments comprised of mixtures of blue (B; 400–500 nm), green (G; 500–600 nm), red (R; 600–700 nm), and far-red (FR; 700–800 nm); warm-white (WW); or equalized-white (EQW) light-emitting diodes. Equations, coefficients of determination (R^2), and p-values are given for linear relationships ($\alpha = 0.05$) under G- (solid lines) and FR-substituted (dashed lines) treatments.

60 μmol·m^{-2}·s^{-1} (Fig. 6). Therefore, B radiation generally did not affect the developmental rate. Lettuce 'Rex' and kale developed one and two more leaves, respectively, under G radiation than under FR radiation at the same photon flux density of 40 or 60 μmol·m^{-2}·s^{-1} (Fig. 6). Chlorophyll concentrations of lettuce 'Rouxai' and kale grown under FR radiation increased as the B photon flux density increased from 0 to 60 μmol·m^{-2}·s^{-1} (Fig. 6). At the same B photon flux density, FR radiation decreased the chlorophyll concentration of all crops more than did G radiation. Compared to $B_{60}R_{120}$, lettuce and kale grown under broadband radiation that included FR (i.e., $B_{20}G_{20}R_{120}FR_{20}$, WW_{180}, and EQW_{180}) had lower chlorophyll concentrations. The foliage color of lettuce 'Rouxai' was darker, redder, and less yellow as the B photon flux density increased from 0 to 60 μmol·m^{-2}·s^{-1} (Fig. 6), indicating higher anthocyanin and chlorophyll concentrations. Interestingly, when 20 μmol·m^{-2}·s^{-1} of B radiation was delivered, its leaves were redder under FR radiation than under the same 40 μmol·m^{-2}·s^{-1} of G radiation.

4. Discussion

The relative growth rate is the product of whole-plant net assimilation and the leaf area ratio (Evans, 1972; Lambers et al., 2008). In this study, changing B, G, or FR radiation did not affect net assimilation

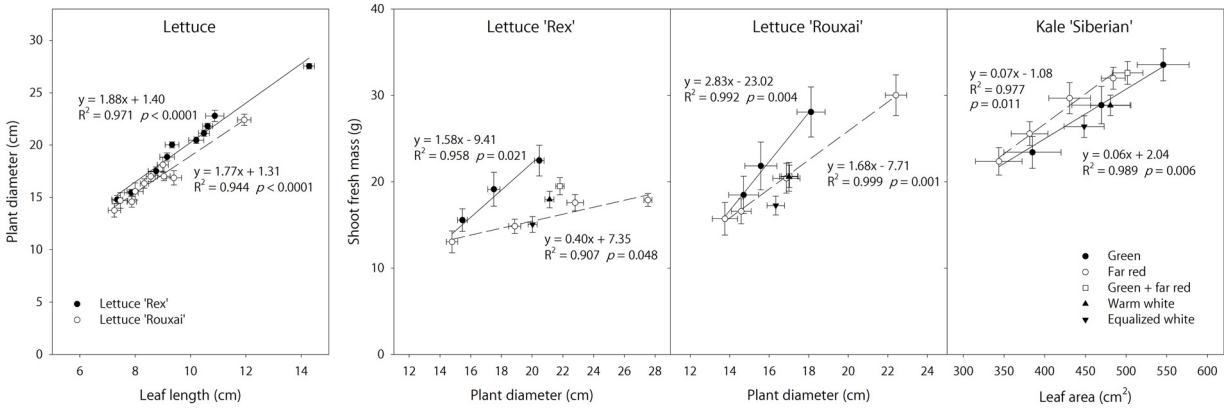

Fig. 5. Relationships between leaf length and plant parameter for lettuce and relationships between plant diameter or leaf area and shoot fresh mass for lettuce and kale. Plants were grown under ten lighting treatments comprised of mixtures of blue (B; 400–500 nm), green (G; 500–600 nm), red (R; 600–700 nm), and far-red (FR; 700–800 nm); warm-white (WW); or equalized-white (EQW) light-emitting diodes. Equations, coefficients of determination (R^2), and p-values are given for linear relationships ($\alpha = 0.05$) for lettuce 'Rex' (solid line) and 'Rouxai' (dashed line) in the left chart or under G- (solid lines) and FR-substituted (dashed lines) treatments in the right chart.

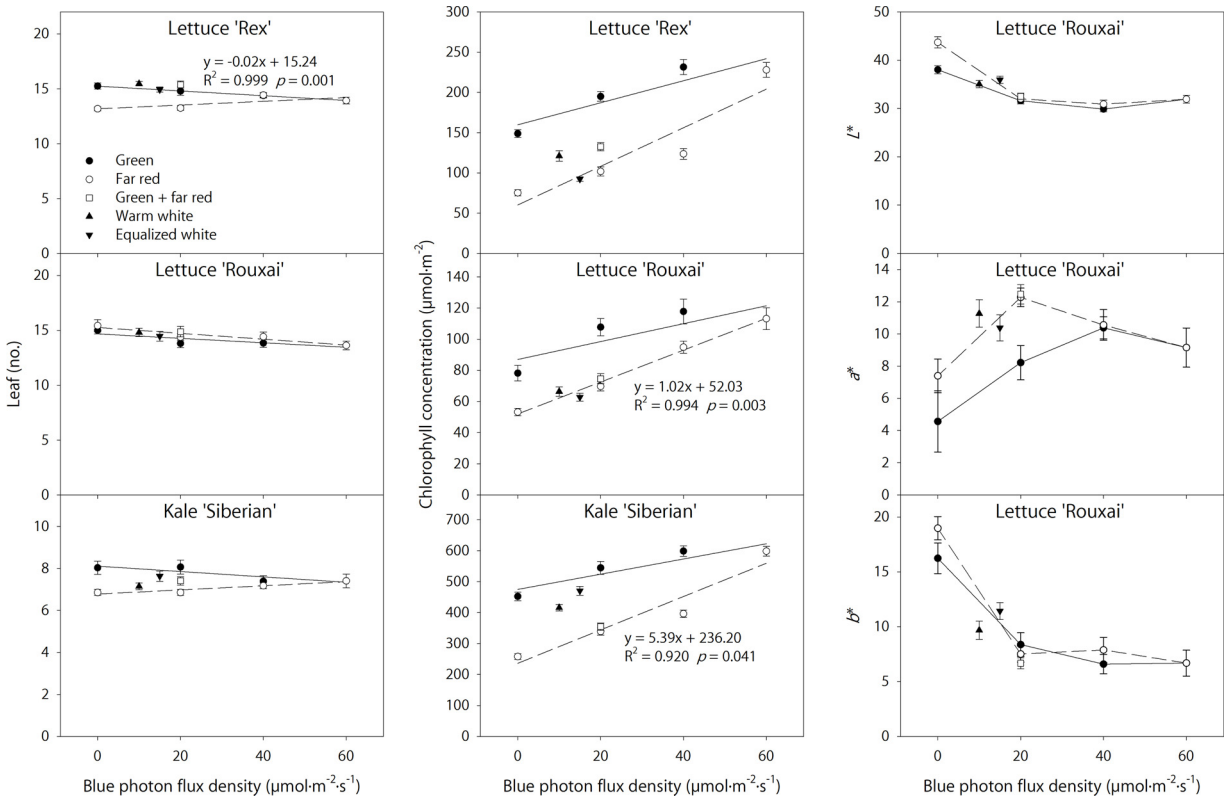

Fig. 6. Leaf number and chlorophyll concentration of lettuce and kale and Lab color space analysis (L*, lightness; a*, green–red; b*, blue–yellow) for foliage coloration of lettuce 'Rouxai'. Plants were grown under ten lighting treatments comprised of mixtures of blue (B; 400–500 nm), green (G; 500–600 nm), red (R; 600–700 nm), and far-red (FR; 700–800 nm); warm-white (WW); or equalized-white (EQW) light-emitting diodes. Equations, coefficients of determination (R^2), and p-values are given for linear relationships ($\alpha = 0.05$) under G- (solid lines) and FR-substituted (dashed lines) treatments.

of kale at a TPFD of 180 μmol·m^{-2}·s^{-1}. Similarly, changing the percentage of B or G radiation generally did not influence net assimilation of various crops at a PPFD of 200 μmol·m^{-2}·s^{-1} (Snowden et al., 2016). On the other hand, the effect of FR radiation on net assimilation of ornamental seedlings was inconsistent; FR radiation either increased or did not influence net assimilation depending on the crop and spectral background (Park and Runkle, 2017, 2018). Our study emphasized relationships between plant morphology and growth as affected by B, G, and FR radiation. We observed positive correlations between leaf size and shoot fresh mass for lettuce and kale. As the leaf area index increases, the fraction of intercepted photosynthetically active radiation increases until a maximum is reached (Maddonni and Otegui, 1996; Wells, 1991). Radiation interception is a major contributor to carbon gain in photosynthesis (Klassen et al., 2003). Therefore, in our study, the increased shoot mass under increasing G or FR radiation (and decreasing B radiation) can at least partly be attributed to increased leaf size and thus, increased radiation interception to drive photosynthesis. Both G and FR radiation can promote extension growth by triggering shade-avoidance responses through photoreceptors (Franklin and Whitelam, 2005; Zhang et al., 2011). A low ratio of R to FR radiation (R:FR) is a typical shade indicator that acts upon phytochromes to promote stem and petiole elongation, leaf expansion, hyponasty, and flowering while reducing branching (Franklin and Whitelam, 2005; Vandenbussche et al., 2005; Park and Runkle, 2017). When plants are exposed to a low R:FR, phytochrome B partially converts to its inactive form and dissociates from phytochrome-interacting factors (PIF) 4 and 5, which then accumulate and promote expression of genes involved in elongation growth (Franklin, 2008). Prolonged exposure to a low R:FR can also increase gibberellin synthesis, which facilitates the functions of PIFs and induces sustained extension growth (Franklin, 2008). In our study, the R:FR decreased as the FR photon flux density increased in a fixed R-radiation background. Leaf length, leaf width, leaf area, plant diameter, and petiole length increased with a decreasing R:FR.

Although G radiation is not absorbed as well as R or B radiation at the upper canopy, it is transmitted further into the canopy. Therefore, the spectral distribution in vegetative shade under sunlight is rich in FR radiation and to a lesser extent, G radiation (Vandenbussche et al., 2005). The addition of 40 μmol·m^{-2}·s^{-1} of G radiation to 90 μmol·m^{-2}·s^{-1} of 44%B + 56%R radiation induced shade-avoidance symptoms including promotion of petiole elongation and hyponasty in wild-type arabidopsis (*Arabidopsis thaliana*) as well as its phytochrome and cryptochrome mutants (Zhang et al., 2011). Although cryptochromes mainly absorb B and ultraviolet-A radiation, they also absorb and respond to G radiation (Liu et al., 2008). Shade-avoidance responses induced by G radiation are likely mediated by cryptochromes, possibly together with an unknown G radiation receptor through a mechanism different from that for FR radiation (Folta, 2004; Zhang et al., 2011; Wang and Folta, 2013). In our study, increasing G and FR radiation (and decreasing B radiation) increased leaf expansion and shoot mass; however, FR radiation sometimes elicited more pronounced shade-avoidance symptoms than did G radiation when delivered at the same photon flux density. The attenuated shade-avoidance response under G radiation can at least partly be attributed to suppression of G-absorbing cryptochromes on expression of shade-induced genes, which is promoted under FR radiation (Zhang et al., 2011; Wang and Folta, 2013).

Besides low R:FR and enriched G radiation, insufficient or low B radiation can also signal shade-avoidance responses through cryptochrome-mediated regulation of PIF4 and PIF5 (Keuskamp et al., 2010; Keller et al., 2011; Pedmale et al., 2016). When B radiation is sufficiently high, cryptochromes in arabidopsis actively suppress PIF4 while cryptochrome 2 and PIF5 are reduced, resulting in normal photomorphogenesis (Pedmale et al., 2016). In contrast, low B radiation allows cryptochromes 1 and 2 to physically interact with and stabilize PIF4 and PIF5, resulting in ample PIF proteins to promote expression of

growth-related genes and increase hypocotyl growth (Pedmale et al., 2016). In our study, the absolute amount of B radiation decreased when B radiation was substituted with G or FR radiation. Therefore, reduced B radiation likely elicited the shade-avoidance symptoms together with increased G or FR radiation. Here, the B photon flux density was not kept constant because we intended to investigate the interaction between B and G radiation at the same TPFD. With an increasing ratio of G to B radiation (G:B), G radiation (peak = 525, 559, or 563 nm) can reverse B radiation effects on various physiological processes, such as hypocotyl elongation and stomatal opening, at least partly by antagonizing degradation of cryptochrome 2 induced by ample B radiation (Folta, 2004; Banerjee et al., 2007; Bouly et al., 2007; Folta and Maruhnich, 2007). A G:B of 2:1 and a peak wavelength of 540 nm were most effective at reversing B-radiation-controlled stomatal opening (Frechilla et al., 2000; Talbott et al., 2002). Although adding G radiation to B + R radiation lowered stomatal conductance of lettuce 'Waldmann's Green', it increased shoot mass rather than limit carbon fixation (Kim et al., 2004b). Our results on lettuce and kale suggest G radiation may antagonize B-radiation-induced inhibition of extension growth, in agreement with previous studies on arabidopsis (Folta, 2004; Bouly et al., 2007).

The inclusion of G radiation in a B + R spectrum can create W radiation and thus improve visual quality for assessment of plant health. White radiation is created by covering B LEDs with a phosphor coating, the material of which influences the W spectrum. The WW and EQW LEDs used in our study had broad spectra covering 400 to 750 nm with predominately R radiation (54%) and G radiation (61%), respectively. Compared with plants grown under 20 $\mu mol \cdot m^{-2} \cdot s^{-1}$ of B radiation, shoot fresh mass was comparable under WW radiation and lower under EQW radiation at an air temperature of 20 °C. However, our unpublished results in a subsequent experiment have shown similar growth of lettuce 'Rouxai' under these two types of W LEDs when the air temperature was 22 °C, indicating a possible interaction between radiation quality and temperature.

There were generally no linear relationships between the B photon flux density and chlorophyll concentrations except under FR radiation for lettuce 'Rouxai' and kale. This suggests radiation interception was mainly determined by leaf expansion and thus total chlorophyll content. Substituting B radiation for FR radiation increased chlorophyll concentrations of lettuce 'Rouxai' and kale. Restricted leaf expansion under increasing B radiation may contribute to elevated chlorophyll concentrations on an area basis. For kale, total chlorophyll content, as estimated by multiplying the chlorophyll concentration and leaf area, showed an increase with increasing B radiation under decreasing FR radiation (data not shown). Response trends were opposite for chlorophyll content and leaf area or shoot mass, suggesting leaf expansion may be a limiting factor in radiation interception. Increased chlorophyll content can be attributed to both increasing R:FR and increasing B radiation. Reduced chlorophyll content is often a shade-avoidance response elicited by low R:FR (Smith and Whitelam, 1997; Franklin, 2008). The active forms (Pfr) of phytochromes A and B interact with PIF1, a transcription factor that represses protochlorophyllide biosynthesis (Huq et al., 2004). Another phytochrome-mediated negative regulator of chlorophyll biosynthesis is PIF3, which interacts with histone deacetylase HDA15 (Liu et al., 2013). Photoactivated phytochromes can inhibit the transcriptional activity of PIF1 and PIF3, thereby promoting light-dependent chlorophyll biosynthesis (Huq et al., 2004; Liu et al., 2013). In our study, increasing the R:FR increased chlorophyll content possibly by increasing repression of PIF1 and PIF3 by the Pfr forms of phytochromes A and B while inhibiting chlorophyll degradation (Okada et al., 1992). Studies on lettuce 'Red Cross' and ornamental seedlings also reported chlorophyll concentrations increased with increasing R:FR (Li and Kubota, 2009; Park and Runkle, 2017, 2018). In addition, B radiation can control accumulation of key Mg-chelatase enzymes, Mg-chelatase subunit H (CHLH) and genomes uncoupled 4 (GUN4), in chlorophyll biosynthesis through phytochrome A and cryptochrome 2 (Stephenson and Terry, 2008). Similar to responses to B radiation in our study, as the fraction of B radiation increased from 0% to approximately 50% in a R-radiation background, chlorophyll concentrations of cucumber (*Cucumis sativus*) 'Hoffmann's Giganta', lettuce 'Sunmang', and lettuce 'Grand Rapids TBR' increased (Hogewoning et al., 2010; Son and Oh, 2013).

Both cryptochromes and phytochromes mediate anthocyanin accumulation. Substituting B radiation for G radiation intensified foliage redness of lettuce 'Rouxai', which was indicative of increased anthocyanin concentrations. Upregulation of anthocyanin accumulation by B radiation is primarily mediated by cryptochrome 1 but requires the presence of functional phytochromes, especially phytochrome B (Ahmad and Cashmore, 1997). The reversal of B effects by G radiation is evident in anthocyanin accumulation of arabidopsis and lettuce 'Red Sails', which is upregulated under B radiation through cryptochrome 1 but reduced by additional G radiation in a fluence-rate-dependent manner (Bouly et al., 2007; Zhang and Folta, 2012; Wang and Folta, 2013). Therefore, increased anthocyanin accumulation under an increasing B:G can at least partly be attributed to both increasing B radiation and decreasing reversal of B effects by G radiation. Besides coaction with cryptochrome 1 under B radiation, phytochromes also play a direct role in anthocyanin biosynthesis under R and FR radiation (Ahmad and Cashmore, 1997; Fankhauser and Casal, 2004). Phytochrome A can be excited by FR radiation to facilitate anthocyanin biosynthesis by suppressing CONSTITUTIVELY PHOTOMORPHOGENIC 1 (COP1), a negative regulator of anthocyanin production that inhibits the transcriptional activity of R2R3 MYELOBLASTOSIS PROTEIN 75 (MYB75) (Li et al., 2014). Responses mediated by phytochrome A were most efficiently elicited by FR radiation notwithstanding the low fraction of active Pfr in the total phytochrome pool (Rausenberger et al., 2011; Zheng et al., 2013). On the other hand, phytochrome B mediates promotion of anthocyanin accumulation under R radiation and its reduction under FR radiation, while photomorphogenesis under FR radiation is mediated predominantly by phytochrome A (Zheng et al., 2013). Decreasing R:FR with or without B radiation increased anthocyanin content in kale 'Red Russian' seedlings (Carvalho and Folta, 2014). The addition of B radiation augmented anthocyanin accumulation under FR radiation (Carvalho and Folta, 2014). Taken together, the deep red coloration of lettuce 'Rouxai' under B + FR radiation (e.g., $B_{20}R_{120}FR_{40}$) can at least partly be attributed to positive regulation of anthocyanin accumulation by both B and FR radiation through cryptochromes and phytochromes.

In conclusion, substituting G and/or FR radiation for B radiation in a fixed R-radiation background increased leaf expansion, radiation interception, and shoot mass of lettuce and kale but reduced chlorophyll concentrations. Increasing G and FR radiation while decreasing B radiation induced shade-avoidance symptoms in control of extension growth and pigmentation; however, FR radiation was sometimes a more potent shade signal than G radiation when delivered at the same photon flux density. The inclusion of G radiation is also useful for creating a visually pleasant W radiation environment, which is relevant for people-plant interactions. However, since discrete G LEDs are inefficient at converting electrical energy to photons, more efficient W LEDs are a suitable alternative to provide G radiation when desired.

Author statement

We confirm that there are no known conflicts of interest associated with this publication, and there has been no significant financial support for this work that could have influenced its outcome.

We confirm that the manuscript has been read and approved by all named authors, and that no other persons who satisfied the criteria for authorship but are not listed. We also confirm that all of us have approved the order of authors listed in the manuscript.

We confirm that we have given due consideration to the protection of intellectual property associated with this work and that there are no

impediments to publication, including the timing of publication, with respect to intellectual property. In so doing, we confirm that we have followed the regulations of our institutions concerning intellectual property.

We further confirm that no experimental animals or human patients have been used in the research reported in this manuscript.

We understand that the Corresponding Author is the sole contact for the Editorial process, including Editorial Manager and direct communications with the office. He is responsible for communicating with the other authors about progress, submissions of revisions, and final approval of proofs. We confirm that we have provided a current, correct E-mail address, which is accessible by the Corresponding Author using the address runkleer@msu.edu.

Declarations of interest

None.

Acknowledgements

We thank David Hamby, Rodrigo Pereyra, Charles Brunault, Alan Sarkisian, and Dorian Spero from OSRAM Innovation for lighting support; Steve Brooks for technical assistance; Randy Beaudry, Dan Brainard, Roberto Lopez, and Emily Merewitz for instruments; and Nathan Kelly, Yujin Park, and Nate DuRussel for experimental assistance. This work was supported by Michigan State University AgBioResearch Project GREEEN GR17-072 and the USDA National Institute of Food and Agriculture, Hatch project 192266.

References

Ahmad, M., Cashmore, A.R., 1997. The blue-light receptor cryptochrome 1 shows functional dependence on phytochrome A or phytochrome B in Arabidopsis thaliana. Plant J. 11, 421–427.

Banerjee, R., Schleicher, E., Meier, S., Viana, R.M., Pokorny, R., Ahmad, M., Bittl, R., Batschauer, A., 2007. The signaling state of *Arabidopsis* cryptochrome 2 contains flavin semiquinone. J. Biol. Chem. 282, 14916–14922.

Bouly, J.P., Schleicher, E., Dionisio-Sese, M., Vandenbussche, F., Van Der Straeten, D., Bakrim, N., Meier, S., Batschauer, A., Galland, P., Bittl, R., Ahmad, M., 2007. Cryptochrome blue light photoreceptors are activated through interconversion of flavin redox states. J. Biol. Chem. 282, 9383–9391.

Brodersen, C.R., Vogelmann, T.C., 2010. Do changes in light direction affect absorption profiles in leaves? Funct. Plant Biol. 37, 403–412.

Carvalho, S.D., Folta, K.M., 2014. Sequential light programs shape kale (*Brassica napus*) sprout appearance and alter metabolic and nutrient content. Hortic. Res. 1, 8.

Evans, G.C., 1972. The Quantitative Analysis of Plant Growth. Blackwell Scientific Publications, Oxford.

Fankhauser, C., Casal, J.J., 2004. Phenotypic characterization of a photomorphogenic mutant. Plant J. 39, 747–760.

Folta, K.M., 2004. Green light stimulates early stem elongation, antagonizing light-mediated growth inhibition. Plant Physiol. 135, 1407–1416.

Folta, K.M., Maruhnich, S.A., 2007. Green light: a signal to slow down or stop. J. Exp. Bot. 58, 3099–3111.

Franklin, K.A., 2008. Shade avoidance. New Phytol. 179, 930–944.

Franklin, K.A., Whitelam, G.C., 2005. Phytochromes and shade-avoidance responses in plants. Ann. Bot. 96, 169–175.

Frechilla, S., Talbott, L.D., Bogomolni, R.A., Zeiger, E., 2000. Reversal of blue light-stimulated stomatal opening by green light. Plant Cell Physiol. 41, 171–176.

Hogewoning, S.W., Trouwborst, G., Maljaars, H., Poorter, H., van Ieperen, W., Harbinson, J., 2010. Blue light dose-responses of leaf photosynthesis, morphology, and chemical composition of *Cucumis sativus* grown under different combinations of red and blue light. J. Exp. Bot. 61, 3107–3117.

Huq, E., Al-Sady, B., Hudson, M., Kim, C., Apel, K., Quail, P.H., 2004. Phytochrome-interacting factor 1 is a critical bHLH regulator of chlorophyll biosynthesis. Science 305, 1937–1941.

Keller, M.M., Jaillais, Y., Pedmale, U.V., Moreno, J.E., Chory, J., Ballaré, C.L., 2011. Cryptochrome 1 and phytochrome B control shade-avoidance responses in Arabidopsis via partially independent hormonal cascades. Plant J. 67, 195–207.

Keuskamp, D.H., Sasidharan, R., Pierik, R., 2010. Physiological regulation and functional significance of shade avoidance responses to neighbors. Plant Signal. Behav. 5, 655–662.

Kim, H.H., Goins, G.D., Wheeler, R.M., Sager, J.C., 2004a. Green-light supplementation for enhanced lettuce growth under red-and blue-light-emitting diodes. HortScience 39, 1617–1622.

Kim, H.H., Goins, G.D., Wheeler, R.M., Sager, J.C., 2004b. Stomatal conductance of lettuce grown under or exposed to different light qualities. Ann. Bot. 94, 691–697.

Klassen, S.P., Ritchie, G., Frantz, J.M., Pinnock, D., Bugbee, B., 2003. Real-time imaging of ground cover: relationships with radiation capture, canopy photosynthesis, and daily growth rate. Digital Imaging and Spectral Techniques: Applications to Precision Agriculture and Crop Physiology, ASA Spec. Publ. 66. ASA, CSSA, and SSSA, Madison, WI, pp. 3–14.

Lambers, H., Chapin, F.S., Pons, T.L., 2008. Growth and allocation. Plant Physiological Ecology. Springer, New York, NY, pp. 312–374.

Li, Q., Kubota, C., 2009. Effects of supplemental light quality on growth and phytochemicals of baby leaf lettuce. Environ. Exp. Bot. 67, 59–64.

Li, T., Jia, K.P., Lian, H.L., Yang, X., Li, L., Yang, H.Q., 2014. Jasmonic acid enhancement of anthocyanin accumulation is dependent on phytochrome A signaling pathway under far-red light in Arabidopsis. Biochem. Biophys. Res. Commun. 454, 78–83.

Liu, H., Yu, X., Li, K., Klejnot, J., Yang, H., Lisiero, D., Lin, C., 2008. Photoexcited CRY2 interacts with CIB1 to regulate transcription and floral initiation in Arabidopsis. Science 322, 1535–1539.

Liu, X., Chen, C.Y., Wang, K.C., Luo, M., Tai, R., Yuan, L., Zhao, M., Yang, S., Tian, G., Cui, Y., Hsieh, H.L., 2013. PHYTOCHROME INTERACTING FACTOR3 associates with the histone deacetylase HDA15 in repression of chlorophyll biosynthesis and photosynthesis in etiolated *Arabidopsis* seedlings. Plant Cell 25, 1258–1273.

Maddonni, G.A., Otegui, M.E., 1996. Leaf area, light interception, and crop development in maize. Field Crops Res. 48, 81–87.

McCree, K.J., 1972. The action spectrum, absorptance and quantum yield of photosynthesis in crop plants. Agric. For. Meteorol. 9, 191–216.

Myers, J., 1971. Enhancement studies in photosynthesis. Annu. Rev. Plant Physiol. Plant Mol. Biol. 22, 289–312.

Okada, K., Inoue, Y., Satoh, K., Katoh, S., 1992. Effects of light on degradation of chlorophyll and proteins during senescence of detached rice leaves. Plant Cell Physiol. 33, 1183–1191.

Park, Y., Runkle, E.S., 2017. Far-red radiation promotes growth of seedlings by increasing leaf expansion and whole-plant net assimilation. Environ. Exp. Bot. 136, 41–49.

Park, Y., Runkle, E.S., 2018. Far-red radiation and photosynthetic photon flux density independently regulate seedling growth but interactively regulate flowering. Environ. Exp. Bot. 155, 206–216.

Parry, C., Blonquist Jr., J.M., Bugbee, B., 2014. *In situ* measurement of leaf chlorophyll concentration: analysis of the optical/absolute relationship. Plant Cell Environ. 37, 2508–2520.

Pedmale, U.V., Huang, S.S.C., Zander, M., Cole, B.J., Hetzel, J., Ljung, K., Reis, P.A., Sridevi, P., Nito, K., Nery, J.R., Ecker, J.R., 2016. Cryptochromes interact directly with PIFs to control plant growth in limiting blue light. Cell 164, 233–245.

Pettai, H., Oja, V., Freiberg, A., Laisk, A., 2005. The long-wavelength limit of plant photosynthesis. FEBS Lett. 579, 4017–4019.

Rausenberger, J., Tscheuschler, A., Nordmeier, W., Wüst, F., Timmer, J., Schäfer, E., Fleck, C., Hiltbrunner, A., 2011. Photoconversion and nuclear trafficking cycles determine phytochrome A's response profile to far-red light. Cell 146, 813–825.

Sager, J.C., Smith, W.O., Edwards, J.L., Cyr, K.L., 1988. Photosynthetic efficiency and phytochrome photoequilibria determination using spectral data. Trans. Am. Soc. Agric. Eng. 31, 1882–1889.

Smith, H., Whitelam, G.C., 1997. The shade avoidance syndrome: multiple responses mediated by multiple phytochromes. Plant Cell Environ. 20, 840–844.

Snowden, M.C., Cope, K.R., Bugbee, B., 2016. Sensitivity of seven diverse species to blue and green light: interactions with photon flux. PLoS One 11 (10), e0163121.

Son, K.H., Oh, M.M., 2013. Leaf shape, growth, and antioxidant phenolic compounds of two lettuce cultivars grown under various combinations of blue and red light-emitting diodes. HortScience 48, 988–995.

Stephenson, P.G., Terry, M.J., 2008. Light signalling pathways regulating the Mg-chelatase branchpoint of chlorophyll synthesis during de-etiolation in Arabidopsis thaliana. Photochem. Photobiol. Sci. 7, 1243–1252.

Sun, J., Nishio, J.N., Vogelmann, T.C., 1998. Green light drives CO_2 fixation deep within leaves. Plant Cell Physiol. 39, 1020–1026.

Talbott, L.D., Nikolova, G., Ortiz, A., Shmayevich, I., Zeiger, E., 2002. Green light reversal of blue-light-stimulated stomatal opening is found in a diversity of plant species. Am. J. Bot. 89, 366–368.

Terashima, I., Fujita, T., Inoue, T., Chow, W.S., Oguchi, R., 2009. Green light drives leaf photosynthesis more efficiently than red light in strong white light: revisiting the enigmatic question of why leaves are green. Plant Cell Physiol. 50, 684–697.

Vandenbussche, F., Pierik, R., Millenaar, F.F., Voesenek, L.A., Van Der Straeten, D., 2005. Reaching out of the shade. Curr. Opin. Plant Biol. 8, 462–468.

Wang, Y., Folta, K.M., 2013. Contributions of green light to plant growth and development. Am. J. Bot. 100, 70–78.

Wells, R., 1991. Soybean growth response to plant density: relationships among canopy photosynthesis, leaf area, and light interception. Crop Sci. 31, 755–761.

Wollaeger, H.M., Runkle, E.S., 2014. Growth of impatiens, petunia, salvia, and tomato seedlings under blue, green, and red light-emitting diodes. HortScience 49, 734–740.

Zhang, T., Folta, K.M., 2012. Green light signaling and adaptive response. Plant Signal. Behav. 7, 75–78.

Zhang, T., Maruhnich, S.A., Folta, K.M., 2011. Green light induces shade avoidance symptoms. Plant Physiol. 157, 1528–1536.

Zhen, S., van Iersel, M.W., 2017. Far-red light is needed for efficient photochemistry and photosynthesis. J. Plant Physiol. 209, 115–122.

Zheng, X., Wu, S., Zhai, H., Zhou, P., Song, M., Su, L., Xi, Y., Li, Z., Cai, Y., Meng, F., Yang, L., 2013. *Arabidopsis* phytochrome B promotes SPA1 nuclear accumulation to repress photomorphogenesis under far-red light. Plant Cell 25, 115–133.